BEHAVIOUR OF NUCLEAR BASS AND WINTHER POTENTIALS TOWARDS THE FUSION SUB-BARRIER CROSS SECTION OF $^{16}O + ^{58,62}Ni$

Nabendu Kumar Deb*, K. Kalita
Department of Physics, Gauhati University, Jalukbari, Guwahati, Assam – 781014, India
*For correspondence. (nd_globe@yahoo.co.in)

Abstract: Six different versions of nuclear Bass and Winther potentials viz., Bass 77, Bass 80, Ngô 80, CW 76, BW 91 and AW 95, are being applied to see the influence of static quadrupole and hexadecapole deformation of targets and its orientations with collision axis on the fusion cross section. The interaction barrier parameters (barrier height, position and its curvature) for the reactions induced by spherical projectiles, ^{16}O, on the slightly deformed targets, $^{58,62}Ni$, have been estimated from the variations of total interaction potential with the inter-nuclear separation; which is then used in Wong's formula to determine the fusion cross section for the reactions. It is found that the nuclear potential considered here strongly depends on the value of the deformation parameters of the target and its orientation. In this work, the experimental fusion cross-section of the reactions $^{16}O + ^{58}Ni$ and $^{16}O + ^{62}Ni$ are investigated with these nuclear potentials. The fusion cross-sections obtained by Bass 80, Ngô 80, BW 91 and CW 76 potentials are found to be in better agreement with the experimental fusion cross-section than that of AW 95 and Bass 77 for the reaction $^{16}O + ^{58}Ni$. On the other hand, for the reaction $^{16}O + ^{62}Ni$, Bass 77, Bass 80 and BW 91 potentials are found out to be in better agreement than AW 95, CW 76 and Ngô 80 in comparison to experimental data.

Keywords: nuclear proximity potential; quadrupole and hexadecapole deformations; interaction barrier parameters; wong's formula; nucleon-nucleon interactions; fusion cross-section

PACS: 02.30.Em, 13.40.Em, 03.65.Xp, 02.30.Rz, 13.75.Cs, 25.60.Pj

1. Introduction.

Heavy ion fusion – fission nuclear reaction studies, especially around the Coulomb barrier, have been a topic of intense research during the past few decades [1, 2]. The fusion cross sections around barrier energies are seen to be influenced dramatically by the internal structure and the entrance channel parameters, namely, the mass asymmetry and the deformation of the interacting nuclei. Such entrance channel properties affect the probability of a compound nucleus system or a dinuclear system significantly. For compound nucleus system, the mass flows from the projectile to the target thereby leading to the formation of compound nucleus which may decay via fission or particle evaporation. For dinuclear system, the mass flows from the target to the projectile and will decay before equilibrating in all degrees of freedom, leading to quasifission. Several authors have studied such entrance channel effect and have proposed different mechanisms of entrance dynamics for different systems [3, 4]. It has been shown both experimentally and theoretically that the fusion cross-section at near barrier energies of spherical, nearly spherical and well-deformed nuclei of either of the colliding partners in the ground state is strongly enhanced by deformation [5]. The quadrupole (β_2) and the hexadecapole (β_4) deformation and the orientation of deformation axis with the colliding axis affect the sub-barrier fusion reactions and hence the fusion barriers, thereby overall affecting the fusion cross-section [1, 6]. Such behaviour can be studied by using the knowledge of nucleus-nucleus interaction potentials which acts as an essential ingredient in these kinds of fusion-fission dynamics. Thus using an orientation dependent nuclear interaction potential, with parabolic approximation, these behaviours are studied here.

Many such nuclear interaction potentials predict the fusion dynamics of a large number of reactions [7]. Among these, widely used phenomenological proximity potential [8] is reported here and is parameterized it within the proximity concept for wider acceptability [7]. With the passage of time, several emendations on original proximity potential [9] have augmented different versions of the same model which can be found in the literature [7].

In this paper, the fusion cross-sections induced by spherical nuclei, ^{16}O, are investigated on slightly deformed and the semi magic target nuclei in the medium mass region, ^{58}Ni and ^{62}Ni, having low deformation parameters, within the theoretical approach, to determine the role of static deformed potentials at sub-barrier energies. The deformation parameters considered here for both the target nuclei are $\beta_2 = 0.093$, $\beta_4 = -0.008$ [10]. Using six different versions of global nuclear proximity potentials, the interaction barrier parameters, viz., the interaction barrier heights, the interaction barrier radii and the interaction barrier curvature, (all being orientation (θ) dependent, where θ is the angle of the symmetric axis of a deformed nucleus with the collision axis) are determined for the two reactions; $^{16}O + ^{58}Ni$ [11] and $^{16}O + ^{62}Ni$ [11]. The fusion cross-sections, obtained after applying these interaction barrier parameters in the Wong's formula for the nucleus – nucleus potential, are then compared with the experimental data to see how well the barriers were reproduced.

2. The Formalism:

2.1. Proximity potential:

Following presents the brief description of the proximity potentials used here in the calculation of fusion barrier parameters and hence fusion cross-sections. The details of the six versions of proximity potential used here are shown in Ref. [7]. The proximity potential is labelled so due to the fact that when the two nuclei approach each other within a distance of few fermi, then additional force acts due to the surface proximity. The proximity force theorem which states that, "the force between two gently curved surfaces in close proximity is proportional to the interaction potential per unit area between the two flat surfaces" forms the basis of the proximity potential. The nuclear part of the interaction potential is taken as the product of a factor depending on the mean curvature of the interaction surface and a universal function (which depends on the separation distance but is independent of colliding nuclei) [12].

2.1.1. Bass 77:

The model Bass 77 [13,14] is based on the assumption of liquid-drop model [15]. Here change in the surface energy of two fragments due to their mutual separation is represented by exponential factor. By multiplying with geometrical arguments, the nuclear part of the interaction potential is written as given in equation (1).

$$V_N(r) = -\bar{R}\Phi(s) \text{ MeV}, \quad (1)$$

where $\left(\bar{R} = \frac{R_1 R_2}{R_1 + R_2}\right)$ and Φ ($s = r - R_1 - R_2$) are the reduced radius and the universal function respectively and r being the distance between the centres of the projectile and the target. In this model, the radii R_1 and R_2 of the interacting nuclei are given as

$$R_i = 1.16A_i^{1/3} - 1.39A_i^{-1/3} \text{ fm}, \; i = 1,2 \quad (2)$$

where A_i is the mass number of the projectile and target.

The universal function is given by the following expression (3)

$$\Phi(s) = \left[0.03\, exp\left(\frac{s}{3.30}\right) + 0.0061\, exp\left(\frac{s}{0.65}\right)\right]^{-1} \text{MeVfm}^{-1} \quad (3)$$

Using the above form, the nuclear part of the interaction potential, $V_N(r)$, given by equation (1) can be calculated.

2.1.2. Bass 80:

The above potential (Bass 77) form was slightly modified by Bass [13] to new one as Bass 1980 (Bass 80) where the radii of the interacting nuclei are modified as following,

$$R_i = R_{si}\left(1 - \frac{0.98}{R_{si}^2}\right) \; i = 1, 2 \quad (4)$$

$$R_{si} = 1.28A_i^{1/3} - 0.76 + 0.8A_i^{-1/3} \text{ fm}, \; i = 1, 2 \quad (5)$$

The universal function for this potential is given by the following expression (6)

$$\Phi(s) = \left[0.033\, exp\left(\frac{s}{3.5}\right) + 0.007\, exp\left(\frac{s}{0.65}\right)\right]^{-1} \text{MeVfm}^{-1} \quad (6)$$

2.1.3. CW 76:

Based on the semi-classical arguments and the recognition that optical-model analysis of elastic scattering

determines the real part of the interaction potential only in the vicinity of a characteristic distance [16–18], Christensen and Winther [19] derived the nucleus-nucleus interaction potential by analyzing the heavy-ion elastic scattering data. The nuclear part of the empirical potential due to Christensen and Winther is given by equation (7)

$$V_N(r) = -A\bar{R}\Phi(s) \text{ MeV} \quad (7)$$

where A is an arbitrary constant, $\left(\bar{R} = \frac{R_1 R_2}{R_1 + R_2}\right)$ and Φ (s = r – R_1 – R_2) are reduced radius and universal function respectively and r is the distance between the centres of the projectile and the target.

According to Christensen and Winther 1976 (referred as CW 76), the constant A = 50,

$$R_i = 1.233A_i^{1/3} - 0.978A_i^{-1/3} \text{ fm} \quad (8)$$

where A_i is the mass number of the projectile and the target and the universal function is given by equation (9),

$$\Phi(s) = exp\left(-\frac{s}{0.63}\right) \quad (9)$$

2.1.4. BW 91:

BW 91 potential is a refined version of the above mentioned potential, CW 76, and was derived by Broglia and Winther [13] in the year 1991 by taking Woods-Saxon parameterization with subsidiary condition of being compatible with the value of the maximum nuclear force predicted by the proximity potential Prox 77 [8],

In this case of BW 91 potential, the nuclear potential $V_N(r)$ remains the same as that of CW 76 which is given by the equation (7). Here the constant A is modified to 'A = 16πγa' where, the diffuseness parameter, a = 0.63 fm and the surface energy coefficient γ is given by

$$\gamma = \gamma_0\left[1 - k_s\left(\frac{N_P - Z_P}{A_P}\right)\left(\frac{N_T - Z_T}{A_T}\right)\right] \quad (10)$$

with γ_0 =0.95 MeV/fm^2 and k_s =1.8. The subscripts P and T refer to the projectile and target respectively. The universal function is written as equation (11) and the expression of the radii of the interacting nuclei is given by the expression (12)

$$\Phi(s) = \left[1 + exp\left(s - \frac{0.29}{0.63}\right)\right]^{-1} \quad (11)$$

$$R_i = 1.233A_i^{1/3} - 0.98A_i^{-1/3} \text{ fm} \quad (12)$$

2.1.5. AW 95:

The parameters a and R_i of the above potential, BW 91, were further refined by Winther to a modified form Aage Winther 1995 (referred as AW 95). These modified parameters are defined in equations (13) and (14) respectively.

$$a = \left[\frac{1}{1.17\left(1+0.53\left(A_1^{\frac{-1}{3}} + A_2^{\frac{-1}{3}}\right)\right)}\right] \text{ fm} \quad (13)$$

$$R_i = 1.20A_i^{1/3} - 0.09 \text{ fm} \quad (14)$$

2.1.6. Ngô 80:

In this model, calculations of the ion-ion potential are performed within the framework of energy-density formalism due to Bruckener *et al.*, using a sudden approximation [20]. Ngô [21] parameterized the nucleus-nucleus interaction potential in line with the proximity concept. The interaction potential is the product of the geometrical factor and a universal function. The nuclear part of the parameterized potential is written as [22]

$$V_N(r) = \overline{R}\Phi(s = r - R_1 - R_2) \text{ MeV} \quad (15)$$

where $\overline{R}$ is the reduced radius [7]. The nuclear radius R_i reads as

$$R_i = \frac{NR_{ni} + ZR_{pi}}{A_i}, i = 1,2 \quad (16)$$

The equivalent sharp radius for protons and neutrons are given as

$$R_{pi} = r_{0_{pi}}A_i^{1/3}; R_{ni} = r_{0_{ni}}A_i^{1/3} \quad 17)$$

with $r_{o_{pi}}$ = 1.128 fm and $r_{o_{ni}}$ = 1.1375 + 1.875 × $10^{-4}$$A_i$ fm

The universal function $\Phi(s = r–R_1–R_2)$ is written in Ref. [7]. This potential is commonly referred as Ngô 80

2.2 Interaction potential:

The total interaction potential is the sum of the centrifugal term, the long range Coulomb repulsive force and the short range nuclear attractive force which is written in equation (18).

$$V(r) = V_C(r) + V_N(r) + \frac{\hbar^2 l(l+1)}{2\mu r^2} \quad (18)$$

where l is the angular momentum quantum number, and μ is the reduced mass of the system. $l = 0$ is considered in this case. The Coulomb potential $V_C(r)$ [12] can be approximated by the relation given in equation (19)

$$V_C(r) = \begin{cases} \frac{Z_P Z_T e^2}{2r_c}\left(3 - \frac{r^2}{r_c^2}\right) & \text{if } r \le r_c \\ \frac{Z_P Z_T e^2}{r} & \text{if } r \ge r_c \end{cases} \quad (19)$$

where Z_P, Z_T are the atomic numbers of the projectile and the target respectively. r is the internuclear separation. Here, the size of the projectile is assumed to be much smaller than the radius of the target, r_c. The nuclear potential V_N (r) is calculated by applying the potentials, viz., Bass 77, Bass 80, CW 76, BW 91, AW 95 and Ngô 80.

The fusion barrier heights and positions for the different potentials mentioned above can be determined by setting the following conditions (20) on the interaction potential determined by the above equation (18).

$$\left.\frac{dV(r)}{dr}\right|_{r=R_b} = 0 \text{ and } \left.\frac{d^2V(r)}{dr^2}\right|_{r=R_b} \le 0 \quad (20)$$

Here, in this paper, a corrected form of the Coulomb barrier is necessary for the deformed target due to which Takigawa's expression [23] is used, i.e.,

$$V_C^1(r) = Z_P Z_T e^2 F^{(0)}(r) + Z_P Z_T e^2 \sum_{\lambda=2,4}\{F_\lambda^{(1)}(r)\beta_\lambda Y_{\lambda 0}(\theta,0)\} + Z_P Z_T e^2 F_{\lambda=2}^{(2)}(r)\frac{5\beta_2^2}{7\sqrt{\pi}} Y_{20}(\theta,0) \quad (21)$$

The first term of this equation (21) is the bare Coulomb interaction, the second and third terms are the linear and the second-order Coulomb couplings respectively. β_2 and β_4 are respectively the quadrupole and the hexadecapole deformation parameters. The linear term is retained only upto the quadrupole and hexadecapole terms, whereas the second-order term is retained only upto the quadrupole term. The expression for the functional forms $F^{(0)}(r)$, $F_\lambda^{(1)}(r)$ and $F_\lambda^{(2)}(r)$ considered here are available in Ref. [12] only for $r > R_T + R_P$, and the system considered here follows this condition as referred in Ref. [23], where R_P and R_T are respectively the radii of the projectile and the target. The fusion cross-sections are calculated by incorporating the interaction barriers so obtained in the Wong model [24].

2.3. Fusion cross-sections:

The model derived by Wong [24] is used here to calculate the fusion cross-sections. The fusion cross-section was calculated by the 'barrier penetration model' under the parabolic approximation [1, 24]. In this formalism, the cross section for complete fusion is given by equation (22)

$$\sigma_f^l(E,\theta) = \frac{\pi(2l+1)}{k^2}\left[1 + exp\left(\frac{2\pi}{\hbar\omega(\theta)}\left(V_B(\theta) - E_{C.M.} + \frac{l(l+1)\hbar^2}{2\pi R_B^2(\theta)}\right)\right)\right]^{-1} \quad (22)$$

where k is the wave number, $E_{C.M.}$ represents the energy in the centre of mass frame; $V_B(\theta)$, $R_B(\theta)$, and ħω are the barrier parameters (barrier heights, barrier radii and barrier curvature respectively) for the different orientations. Considering the value of $l = 0$, the fusion cross-sections at each angle reduces to

$\sigma_f(E,\theta) = \sum_l \sigma_f^l(E,\theta)$

$$= \frac{10R_B^2(\theta)\hbar\omega(\theta)}{2E_{C.M.}} ln\left[1 + exp\left[\frac{2\pi(E_{C.M.} - V_B(\theta))}{\hbar\omega(\theta)}\right]\right] \quad (23)$$

Finally, the total cross-section (equation (24)) is given by integration over the angles

$$\sigma_f(E) = \int_0^{\frac{\pi}{2}} \sigma_f(E,\theta)d\theta. \quad (24)$$

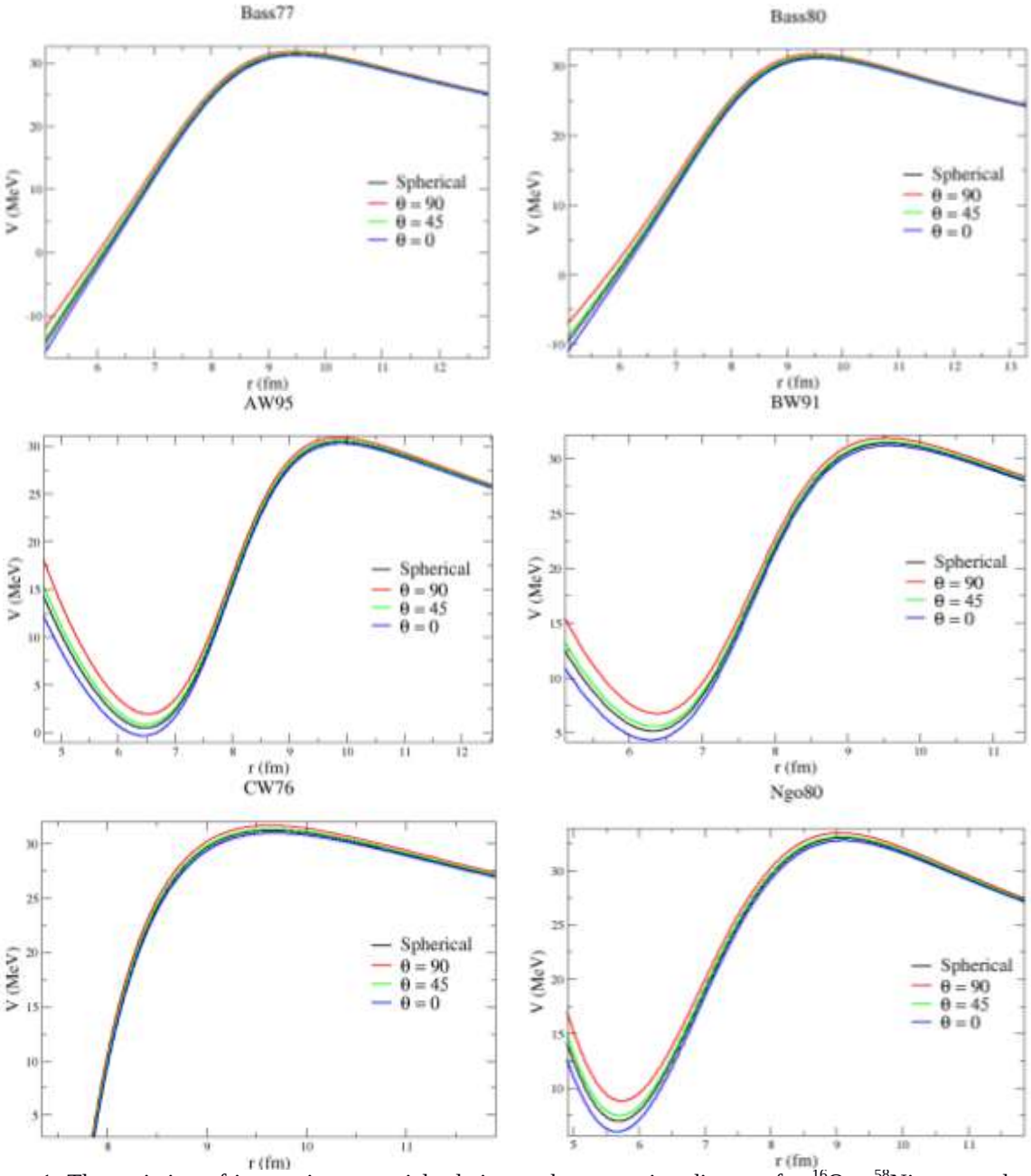

Figure 1: The variation of interaction potential relative to the separation distance for $^{16}O + ^{58}Ni$ system due to six different proximity potential as mentioned accordingly in the plot assuming spherical and deformed target (including only Coulomb correction) at typical orientations as indicated.

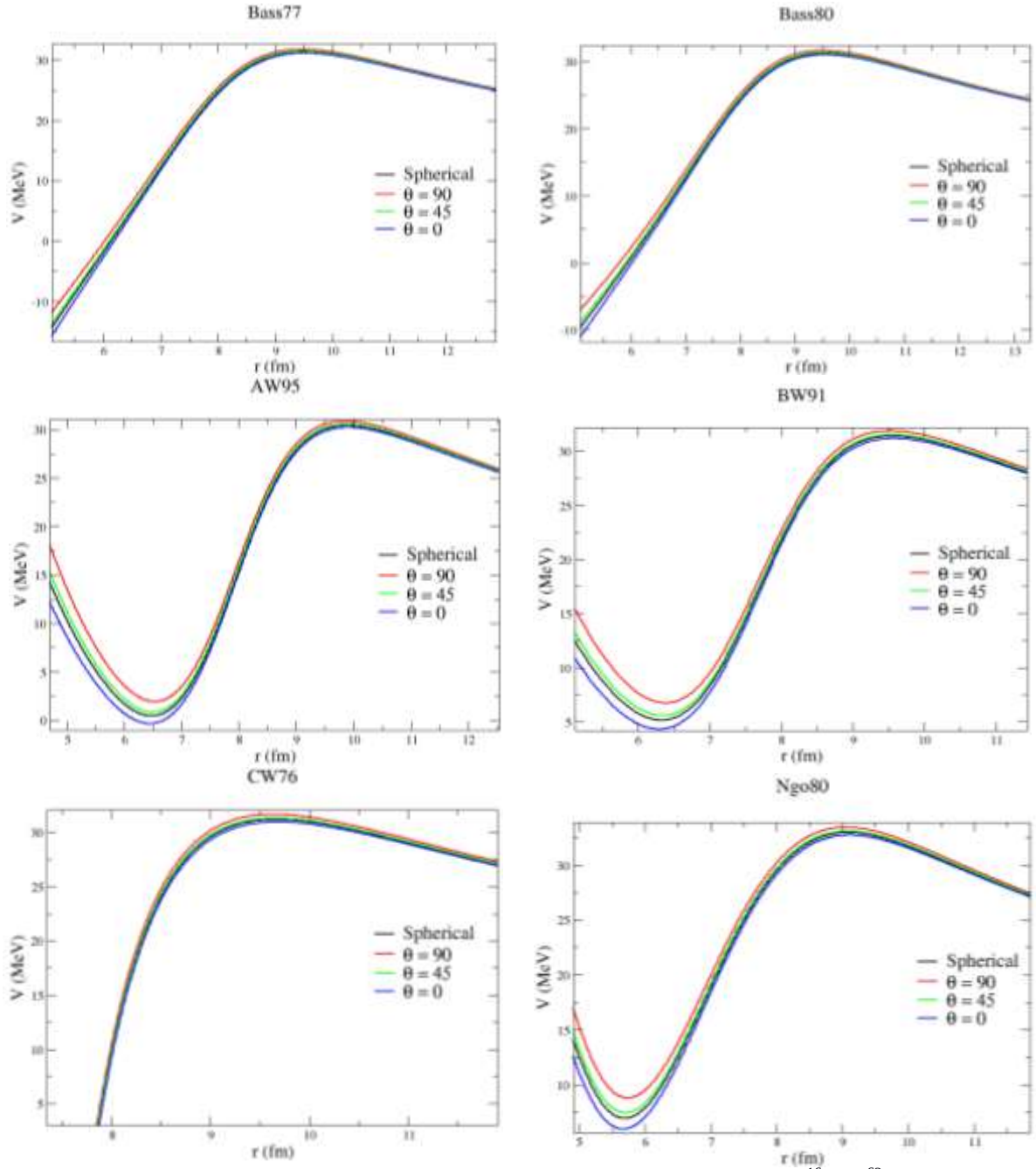

Figure 2: The variation of interaction potential relative to the separation distance for $^{16}O + ^{62}Ni$ system due to six different proximity potential as mentioned accordingly in the plot assuming spherical and deformed target (including only Coulomb correction) at typical orientations as indicated.

3. Results and discussions:

The total interaction potential V (MeV) as a function of internuclear distance r (fm) for few orientations (say 0, 45, 90 degrees) for the two reactions, i.e., $^{16}O + ^{58}Ni$ (Fig. 1) and $^{16}O + ^{62}Ni$ (Fig. 2) are obtained using the six proximity potentials, i.e., Bass 77, Bass 80, CW 76, BW 91, AW 95 and Ngô 80. In these figures, x- axis corresponds to the distance between the interacting nuclei and y-axis corresponds to the interaction potential. Due to the slightly deformed target, the corrected form of Coulomb and nuclear part of the total potential is applied here. The effective orientation dependent interaction potential is then calculated over all these plausible orientations from 0 – 90 degrees, the deformation being axially symmetric. Fig. 1 and Fig. 2 shows the curve for the $^{16}O + ^{58}Ni$ and $^{16}O + ^{62}Ni$ systems respectively due to all six proximity potentials. It can be seen in the figure

that there is a slight change in the total interaction potential. The shape of the curve is raised slightly for the potential due to deformation as is evident in the figures. It is observed from the curve that the target deformation produces the more repulsive potential at shorter distances. At distance below the barrier radius (R_B) a potential pocket exists which is expected. For distances greater than R_B the spherical and deformed cases reveal almost the same behaviour revealing the insensitiveness of the potential expression at larger distance. Hence the potential, whether due to deformed nuclei or spherical nuclei, shows almost the same behaviour at larger internuclear separation by nearly merging with each other. However for the potentials CW 76 even at closer distances, lesser than R_B, there is no change in behaviour because of deformed nuclei or spherical nuclei. This is mainly due to the exponential nature of the nuclear potential. As such, in this case, the change in nuclear potential overrides the change in Coulomb potential [12].

Table 1: Barrier parameter for the two systems after applying Coulomb correction.

Potentials	$^{16}O + ^{58}Ni$						$^{16}O + ^{62}Ni$					
	90^0		45^0		0^0		90^0		45^0		0^0	
	V_B (MeV)	R_B (fm)	V_B (MeV)	R_B (fm)	V_B (MeV)	R_B (fm)	V_B (MeV)	R_B (fm)	V_B (MeV)	R_B (fm)	V_B (MeV)	R_B (fm)
Bass 77	32.1	9.4	31.5	9.5	31.3	9.6	31.8	9.5	31.5	9.5	31.2	9.5
Bass 80	31.8	9.1	32.4	9.1	31.3	9.6	31.7	9.5	31.4	9.5	31.1	9.5
CW 76	30.6	9.4	31.6	9.5	30.8	9.6	31.6	9.6	31.3	9.7	30.9	9.7
BW 91	31.8	9.3	31.6	9.6	31.3	9.5	31.9	9.5	31.5	9.5	31.2	9.6
AW 95	30.8	9.7	30.4	9.8	30.3	9.8	30.9	9.9	30.5	9.9	30.2	9.9
Ngô 80	33.4	9.3	33.1	9.4	32.5	9.3	33.4	9.1	33.1	9.1	32.7	9.1

The interaction barrier parameters value are then obtained (as tabulated in table 1) after applying successive Coulomb corrections due to the quadrupole and hexadecapole term (linear-order) and the quadrupole term (second-order) at these orientations for the two reactions. The barrier parameters, so obtained, are then applied in Wong's formula, to analytically calculate the fusion cross-sections for these systems and compared with the corresponding experimental cross-sections for $^{16}O + ^{58}Ni$ and $^{16}O + ^{62}Ni$ [11] systems as is shown in Fig. 3. Both the systems have shown some enhancement in the sub-barrier region compared to the barrier penetration model in one dimensional mode. This is attributed to the inelastic coupling of the interacting nuclei by N. Keelay et al. [11]. In this case, as the target nuclei are slightly deformed, the deformed potentials are used to study the sub-barrier cross section of these reactions in view of deformation. For $^{16}O + ^{58}Ni$, except AW 95 which overestimates the experimental data, rest of the potentials give better results at above barrier energies and in the sub-barrier region. But towards the deep sub-barrier regions, except AW 95, which overestimate the data to a great extent, all other potentials overestimate the data to a certain extent. Ngô 80 is nearest to the experimental data in the sub-barrier region. Even for $^{16}O + ^{62}Ni$, except AW 95 which overestimates the experimental data throughout, rest of the potentials give better results at above barrier energies. But in the sub-barrier region, Bass 77, Bass 80 and BW 91 appear to be closer to the experimental data although except AW 95 all the other potentials underestimate the data. Thus, overall, the fusion-cross section for the Bass 77, Bass 80 and BW91 are found to be better in reproducing the same compared to that of AW 95, CW 76 and Ngô 80 for the reaction $^{16}O + ^{62}Ni$ and the fusion-cross section for the Bass 77, Bass 80, BW91 and Ngô 80 are found to be better in reproducing the same compared to that of AW 95 and CW 76 for the reaction $^{16}O + ^{58}Ni$. These deviations of the fusion cross section obtained due to the nuclear proximity potential from that of the experimental results may be attributed to the fact that the coulomb potentials considered here are orientation dependent, but nuclear potentials considered here is spherical. Thus some modifications are required in the nuclear proximity potentials' expression considered here in terms of orientation.

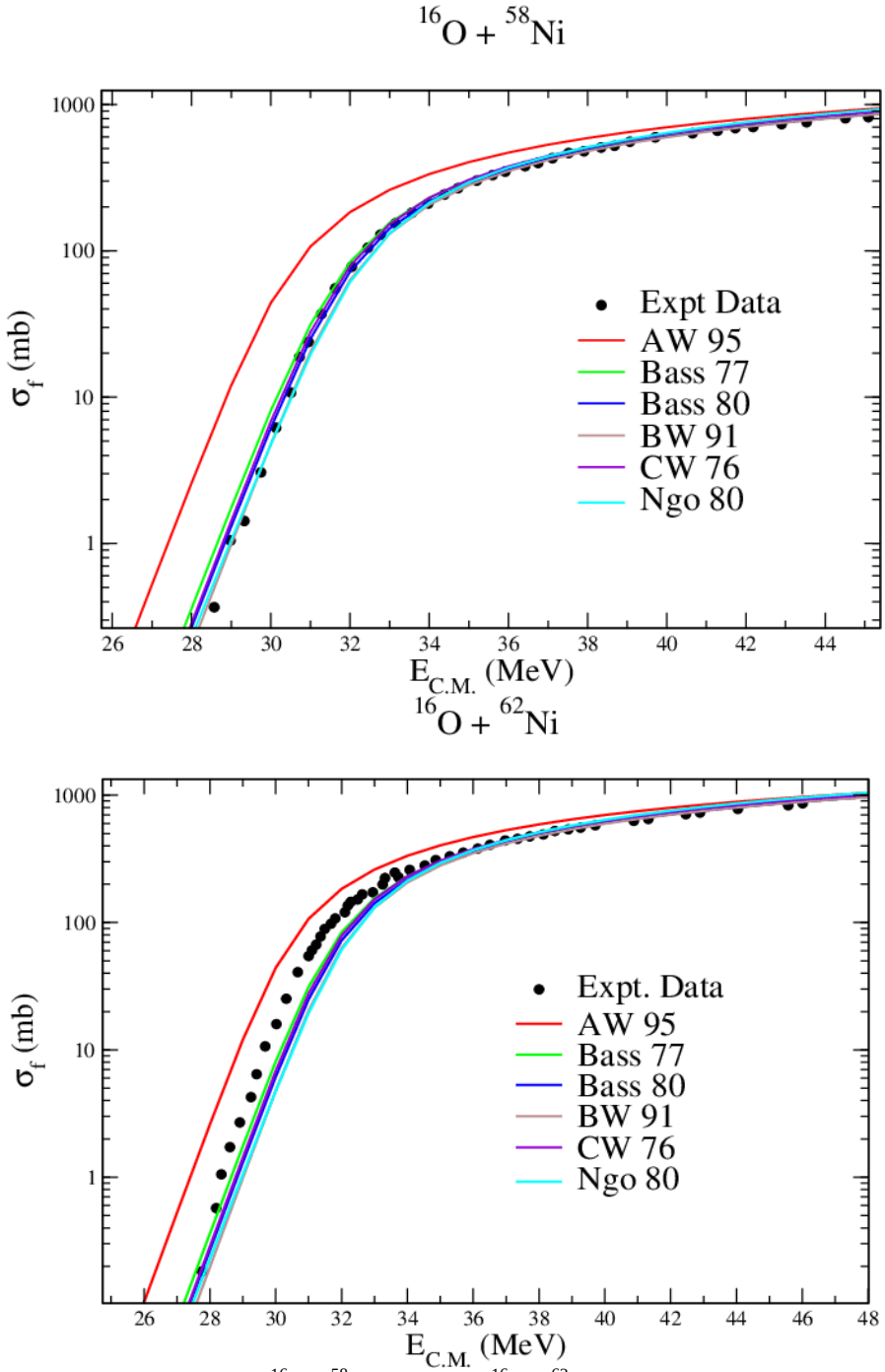

Figure 3: The fusion cross-sections of $^{16}O+ ^{58}Ni$ (top) and $^{16}O+ ^{62}Ni$ (bottom) with relative to centre of mass energy. The experimental data is obtained from Ref. [11].

4. Conclusion:

The effects of target deformation and its orientation with the collision axis on fusion barriers of the reactions $^{16}O + ^{58}Ni$ and $^{16}O + ^{62}Ni$ are seen by employing six versions of different proximity-based orientation dependent interaction potentials as the barrier parameters are orientation dependent. The fusion cross-sections so obtained due to Bass 77, Bass 80, BW91 and Ngô 80 potentials showed good agreement with the experimental data at both sub-barrier and above barrier energies; but overall, Bass 77, Bass 80 and BW91 potentials seems to be in stronger agreement. The deviation of fusion cross-sections from the experimental data may be due to the fact that both Coulomb and nuclear corrections are needed for all the proximity potentials. In this work, the total interaction potential is extracted by considering the Coulomb corrections for all the potentials. To see the

deformation effect on fusion cross-section around the barriers, more sophisticated experimental data are required.

Acknowledgement:

The authors gratefully acknowledge the Council of Scientific and Industrial research (CSIR), New Delhi for the award of JRF.

References:

[1] C. J. Lin, J. Xu, H. Zhang, Z. Liu, F. Yang and L. Lu, Phys. Rev. C 63, 064606, 2001.
[2] A. Balantekin and N. Takigawa, Rev. Mod. Phys. 70, 77, 1988.
[3] P. D. Shildling, N. Madhavan, V.S. Ramamurthy, S. Nath, N.M. Badiger, Santanu Pal, A.K. Sinha, A. Jhingan, S. Muralithar, P. Sugathan, S. Kailas, B.R. Behera, R. Singh, K.M. Varier and M.C. Radhakrishna, Phys. Lett. B 670, 99, 2008.
[4] E. Prasad, K.M. Varier, R. G. Thomas, P. Sugathan, A. Jhingan, N. Madhavan, B. R. S. Babu, Rohit Sandal, S. Kalkal, S. Appannababu, J. Gehlot, K. S. Golda, S. Nath, A. M. Vinodkumar, B. P. Ajithkumar, B. V. John, G. Mohanto, M. M. Musthafa, R. Singh, A. K. Sinha and S. Kailas, Phys. Rev. C 81, 054608, 2010.
[5] J. O. Fernandez Niello and C. Dasso, Phys. Rev. C 39, 2069, 1989.
[6] M. Ismail, W. Seif and M. Botros, Nucl. Phys. A 828, 333, 2009.
[7] I. Dutt and R. Puri, Phys. Rev. C 81, 064608, 2010; Phys. Rev. C 81, 064609, 2010; Phys. Rev. C 81, 044615, 2010.
[8] J. Blocki, J. Randrup, W. Swiatecki and C. F. Tsang, Ann. Phys. 105, 427, 1977.
[9] W. D. Myers and W. Swiatecki, Phys. Rev. C 62, 044610, 2010.
[10] G. Lalazissis, S. Raman and P. Ring, Atomic Data and Nuclear Data Tables 71, 1, 1999.
[11] N. Keeley, J. S. Lilley, J. X. Wei, M. Dasgupta, D. J. Hinde, J. R. Leigh, J. C. Mein, C. R. Morton, H. Timmers and N. Rowley, Nucl. Phys., A 628, 1, 1998.
[12] T. Rajbongshi and K. Kalita, Cent. Eur. J. Phys. 12 (6), 433, 2014.
[13] W. Reisdorf, J. Phys. G: Nucl. Part. Phys. 20, 1297, 1994.
[14] R. Bass, Phys. Rev. Lett. 39, 265, 1977.
[15] R. Bass, Phys. Lett. B 47, 139, 1973.
[16] R. A. Broglia and A. Winther, Heavy Ion Reactions, Parts I and II, Frontiers in Physics, vol. 84 (Addison-Wesley, Boston, US), 1991.
[17] O. Akyuz and A. Winther, In: R. A. Broglia, C. H. Dasso and R. Ricci, (Eds.), Proc. Enrico Fermi International School of Physics 1979, 443, North-Holland, Amsterdam, 1981.
[18] A. Winther, Nucl. Phys. A 594, 203, 1995.
[19] P. R. Christensen and A. Winther, Phys. Lett. B 65, 19, 1976.
[20] K. A. Brueckner, J. R. Buchler and M. Kelly, Phys. Rev. 173, 944, 1968.
[21] H. Ngô and C. Ngô, Nucl. Phys. A 348, 140, 1980.
[22] G. Royer and R. Rousseau, Eur. Phys. J. A 42, 541, 2009.
[23] N. Takigawa, T. Rumin and N. Ihara, Phys. Rev. C 61, 044607, 2000.
[24] C. Y. Wong, Phys. Rev. Lett. 31, 766, 1973.